Fibers and Polymers 2014, Vol.15, No.11, 2283-2289 DOI 10.1007/s12221-014-2283-4

Fabrication of Nanofibers with Ultrahigh Production by a Facile High Pressure Air-jet Atomized Electrospinning

Jianxin He[1,2]*, Lidan Wang[1], Rangtong Liu[1,2], Mingjun Zhang[1], Weilin Tan[1], and Yanchao Wu[1]

[1]*College of Textiles, Zhongyuan University of Technology, Zhengzhou 450007, P.R. China*
[2]*Key Laboratory of Functional Textile Materials of Henan Province, Zhongyuan University of Technology, Zhengzhou 450007, P.R. China*

(Received March 15, 2014; Revised June 10, 2014; Accepted June 16, 2014)

Abstract: A novel method named as high pressure air-jet atomized electrospinning was proposed to prepare nanofibers with ultrahigh production. The spinning solution with lower concentration and viscosity was cutted into micron-sized droplets by a 700 mesh filter in the front of nozzle and then was crushed and atomized into massive smaller droplets, which were drawn into nanofibers directly under the electric force and airflow force. Flow field under different air pressure was simulated to study its effect on the formation of nanofibers. The airflow showed the minimum pressure and maximum velocity at a location 2 cm away from the spray nozzle, where small droplets cutted were crushed and atomized into massive smaller droplets by the converging airflow. The velocity and distribution region of the airflow increased with increasing air pressure. It showed a smaller diameter of 150 nm and ultrahigh production of 75.6 g/h for nanofibers prepared based on this novel method at the air pressure of 0.8 MPa. The production of nanofibers almost reached thousands of times of that from conventional needle electrospinning.

Keywords: Nanofibers, Electrospinning, Flow field, Atomization

Introduction

Electrospun nanofibers have been applied widely on many fields such as textile and garment, tissue scaffolds, electronic device, filtration, medical and health due to their ultrafine scale, high specific surface area, as well as the unique porous structure [1-3]. However, the lower yield restricts the industrialization of conventional needle electrospinning.

Currently, a number of synthesis methods have been demonstrated for improving the output of nanofibers, including multi-needle and needleless systems [4]. For the former, the production of nanofibers was improved by increasing the number of needles. However, problems of interference between jets due to the resultant electric forces and clogging needle could not be avoided [5]. Many studies have indicated that a higher production can be achieved using needleless systems [6-8], including porous electrospinning [9], sputtering electrospinning [10], bubble electrospinning [11], cleft electrospinning [12] and electro-centrifugal spinning [13].

Recently, some researchers have prepared electrospun nanofibers using blowing-assisted electrospinning. Yao and Wu [14] demonstrated a unique blowing-assisted electrospinning process that blowed air around the spinneret, to get a uniform polysulfone nanofibers under the combination of air blowing-induced shear force and the electrostatic force. Tudorel *et al.* [15] used a modified rotary-jet spinning system, which allowed a forced air flow produced by an air compressor to interfere with the polymer jets, to obtain parallel polymer fibers. The distribution of fiber diameters was varying between nanometer scales in the case of pure polyurethane. Hou *et al.* [16] prepared PMDA/ODA polyimide nanofiber membranes by using the blowing-assisted electrospinning. The overall flow rate of spinning solution was 10 m*l*/h and the production of nanofibers was 0.5-0.8 g/h. Hsiao *et al.* [17] developed a blowing-assisted multiple-jet electrospinning setup for preparing electrospun polycarbonate nanofibers. The feed rate of polymer solution for six needles was up to 3.0 m*l*/h. Eduard *et al.* [18] designed a gas-assisted melt electrospinning setup, where a heated gas stream was applied to one of two (or multiple) co-axial jets, raising the temperature of spinning jet movement area and preventing the polymer from solidifying near the nozzle in order to produce thinner fibers. Airflow used in these methods of preparing nanofibers was to provide additional drawing force or assist nanofibers alignment. However, the production of nanofibers was improved only dozens of times.

Here, a novel method applying air-jet, named as high pressure air-jet atomized electrospinning was proposed to prepare nanofibers with ultrahigh production. This method adopted spinning solution with lower concentration and viscosity, which was easily cutted into micron-sized droplets by a 700 mesh filter in the front of nozzle and then was crushed and atomized into massive smaller droplets by the high-speed airflow. Finally, nanofibers were formed through drawing these smaller droplets directly under the electric force and airflow force.

Experimental

Preparation of Spinning Solution

PAN solution with 7 wt% concentration was prepared

*Corresponding author: hejianxin771117@163.com

through dissolving PAN powder (M_W=600,000) in N-N dimethyl formamide (DMF) solution at 80 °C for 4 h.

Electrospinning

The set-up of high pressure air-jet atomized electrospinning is shown in Figure 1, including a DC power apply, spray gun, air compressor, solution reservoir, metering pump and collector. During experiment, compressed air was fed into the spray gun by air compressor. PAN solution was transported to nozzle with uniform rate through metering pump and then was divided into smaller droplets by a 700 mesh filter with 20 μm diameter in front of the nozzle. These droplets were atomized by the high-speed air and then became nanofibers based on the double effect of electric field and flow field. A voltage of 30 kV was applied to the nozzle and nanofibers were collected at a location 60 cm away from the spray nozzle. The overall flow rate of spinning solution was 1500 m*l*/h.

Flow Field Simulation

Flow field simulation uses the standard k-ε turbulence model. An unstructured mesh is used to mesh the entire region and the structure of the nozzle is simplified in order to reduce meshing time. The spinning nozzle is simplified to a cylinder that consists of two hollow ones with a height of 0.005 m and the base diameter 0.007 m and 0.005 m, respectively. The airflow movement space is simplified to a cuboid with 0.8 m long, 0.6 m wide and 0.6 m high. The pressure inlet boundary condition is applied to the inlet of the spinning nozzle, that is, inlet pressure is air pressure of 0.4 MPa, 0.6 MPa and 0.8 MPa respectively. The pressure outlet boundary is applied to the nozzle outlet, that is , outlet pressure is standard atmospheric pressure (1.01×10^5). All the solid walls in the calculated area use a no-slip boundary condition.

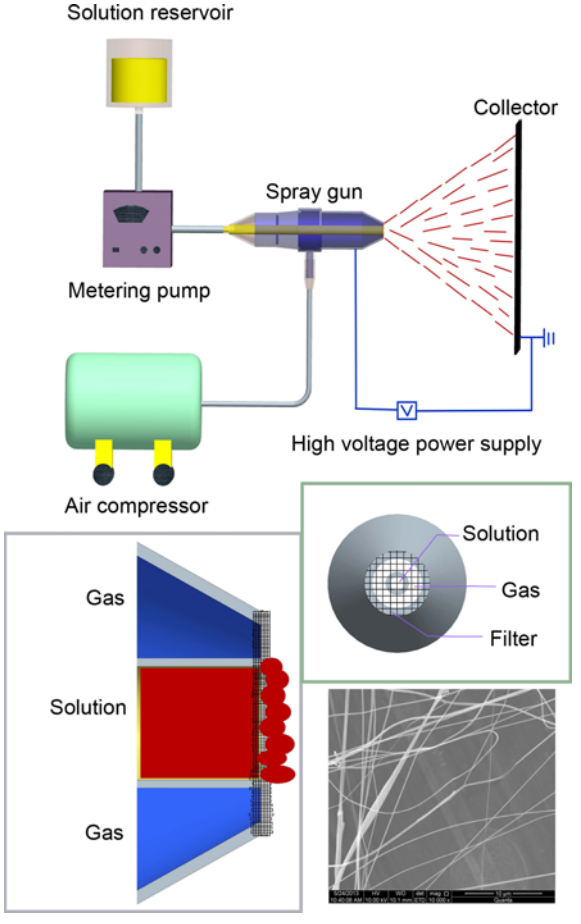

Figure 1. Schematic of the novel high pressure air-jet atomized electrospinning set-up.

Fiber Morphology

Nanofibers collected were coated with gold film in order to observe fiber morphologies. The instrument was a JEOL JSM-5600LV electron microscopic with an accelerating voltage of 15 kV. The diameters of fibers were calculated based on the SEM images. At least 100 counts were taken for each measurement.

Results and Discussion

Flow Field Simulation

The airflow distributions around the nozzle were simulated by FLUENT software, as shown in Figure 2.

Figure 2(A) is the velocity vector plot around the nozzle, in which arrows denote the direction of velocity. The airflow velocity shows the highest value at the jet orifice outlet and then decreases rapidly after the air flows into the movement region. There is an airflow converging point at a distance of 2 cm from the nozzle, at the same time, a swirling airflow appears behind the point. Then the converging airflow expands forward. It can be divided into four sections according to characteristics of the airflow.

The airflow velocity achieves the highest value but the pressure is minimum in section C where airflow converges, except section A at the nozzle. Air pressure gradually increases up to the normal atmospheric pressure, and airflow velocity gradually reduces in region D in front of the converging point. Figure 3 shows the airflow velocity distribution along the central axis, from which it can be seen that the airflow velocity reaches to the maximum value at a distance of 2 cm from the nozzle due to airflow converging and then decreases gradually.

Therefore, the micron-sized droplets obtained through filter cutting would enter section B to be dispersed by the swirling airflow and then enter section C to be crushed and atomized into smaller droplets by the converging airflow. Massive smaller droplets would be drawn into nanofibers directly under the electric force and airflow force.

The contours of airflow velocity under different air pressure in the whole spinning region are shown in Figure 4. The coverage area of airflow expands with air pressure increasing.

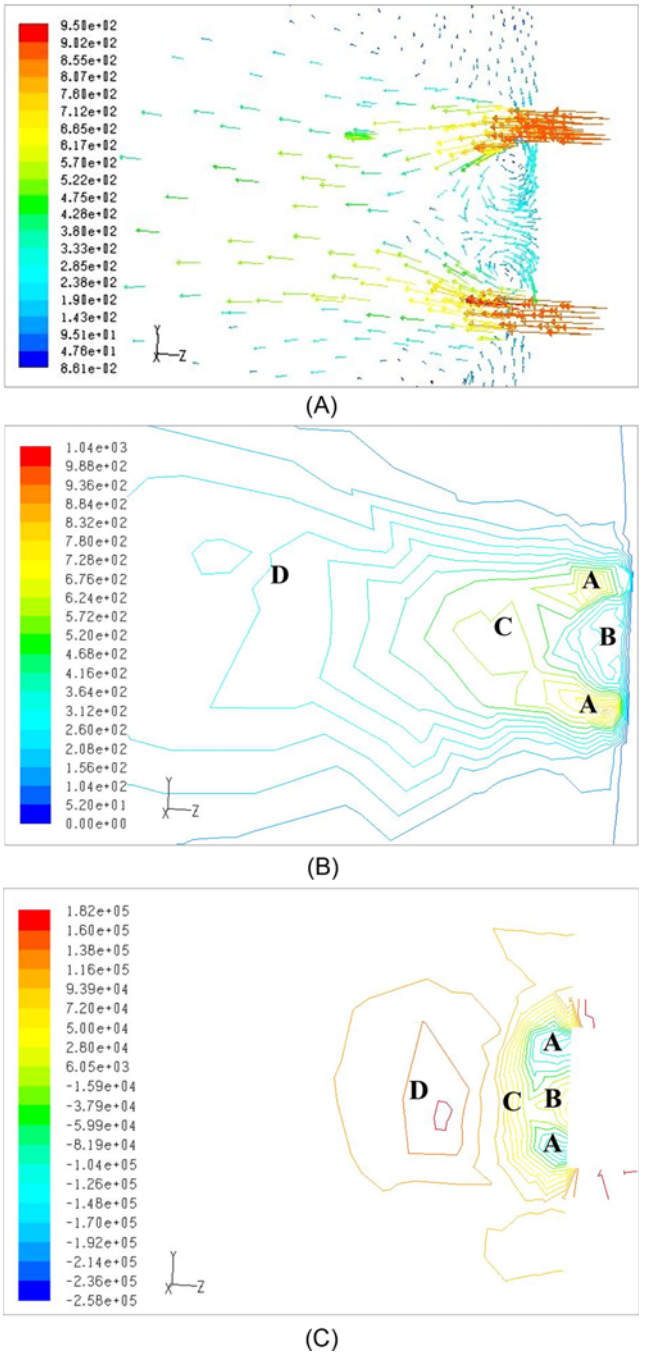

Figure 2. The airflow distribution in front of the nozzle; (A) velocity vectors plot of the airflow, (B) velocity magnitude contours of the airflow, and (C) static pressure distribution of the airflow.

Obviously, the deposition of nanofibers and moving region of spinning jet would be affected.

Jet and Fiber Deposition

The experiment process of preparing nanofibers is shown in Figure 5. A conical atomization region containing solution jet presented between the nozzle and collector. The cone angle and contrast of the atomization region increased with increasing air pressure, indicating that higher air pressure expanded the movement region of spinning jet and increased the density of spinning jet. When the flow rate, applied voltage and collection distance were constant, the higher air pressure, the stronger the airflow. Thus, the effect of atomization and crushing on the spinning solution would be strengthen, promoting more nanofibers to be obtained from massive smaller droplets. When 0.8 MPa air pressure was provided, nanofibers showed a maximum deposition area with production of 75.6 g/h (Table 1). Through our research, we can know that when the flow rate is constant, some large droplets atomized deficiently dropped in the region between the nozzle and collector under lower air pressure. Therefore, more droplets atomized and drafted into nanofibers and reached the collector with the increasing of the air pressure.

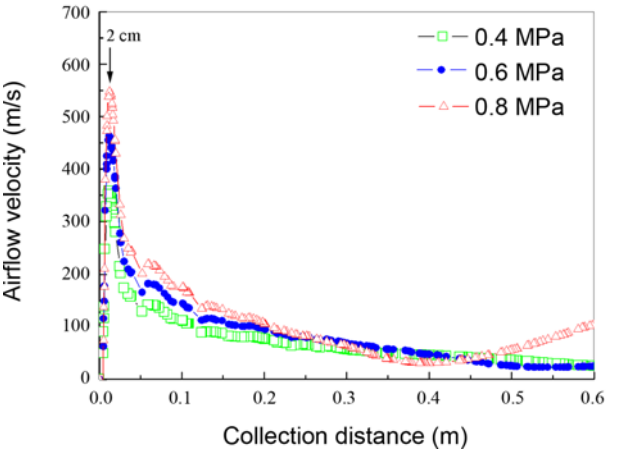

Figure 3. Velocity distribution along the central axis.

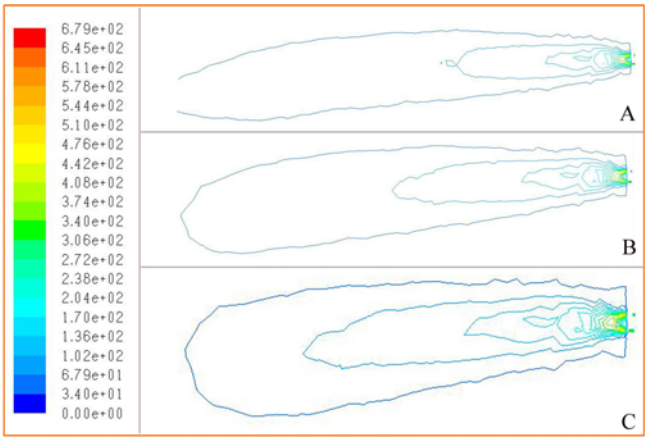

Figure 4. Velocity magnitude contours of the airflow between the nozzle and collector at the air pressure of (A) 0.4 MPa, (B) 0.6 MPa, and (C) 0.8 MPa.

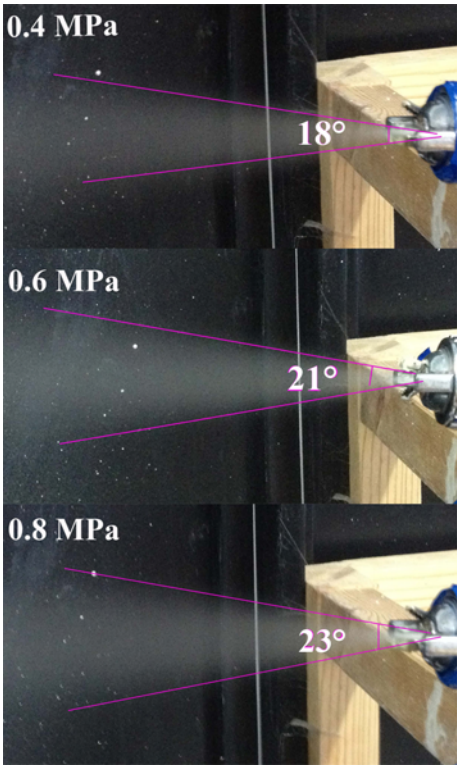

Figure 5. The experiment photographs of high pressure air-jet atomized electrospinning.

Table 1. Production and deposition area of nanofiber mats under different air pressure

Air pressure (MPa)	Area (cm^2)	Production (g/h)
0.4	994.8	33.4
0.6	1533.6	65.4
0.8	2073.9	75.6

The nanofibers depositions under different air pressure are shown in Figure 6. When the air pressure was more than 0.6 MPa, fiber deposition area consisted of three parts, namely hollow region, dense region and rarefied zone. High air pressure can bring about greater impact force, which had a significant influence on the fiber receiving. The airflow still kept a higher speed along the central axis after its converging at a distance of 2 cm from the nozzle. The collector suffered an impact force from the high-speed air jet around the central axis, leading to the formation of hollow region with only little nanofibers. However, the hollow region in the center of the deposition area disappeared due to a relatively lower air pressure under 0.4 MPa air pressure. This was because when the air pressure was lower than 0.4 MPa, the spinning solution could not be fully atomized to droplets and most of the droplets could not reach the collector. On the other hand, high impact force seriously affected the receiving of the nanofibers.

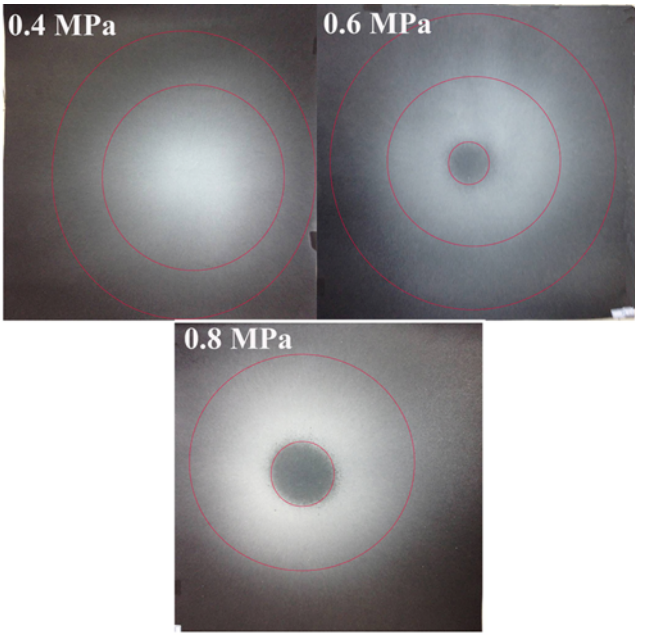

Figure 6. Nanofiber depositions under different air pressure.

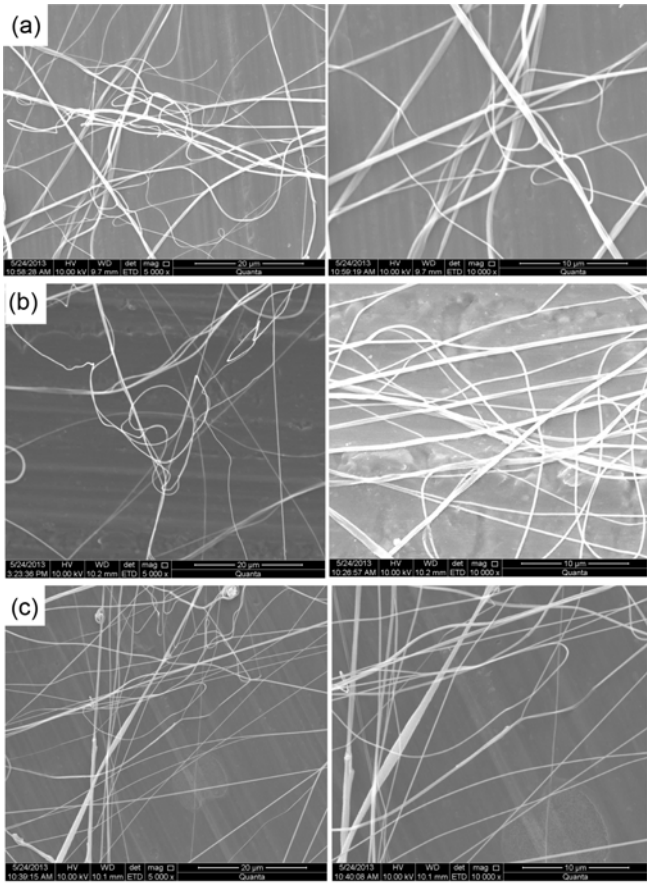

Figure 7. SEM photographs of the nanofibers obtained under the air pressure of (a) 0.4 MPa, (b) 0.6 MPa, and (c) 0.8 MPa.

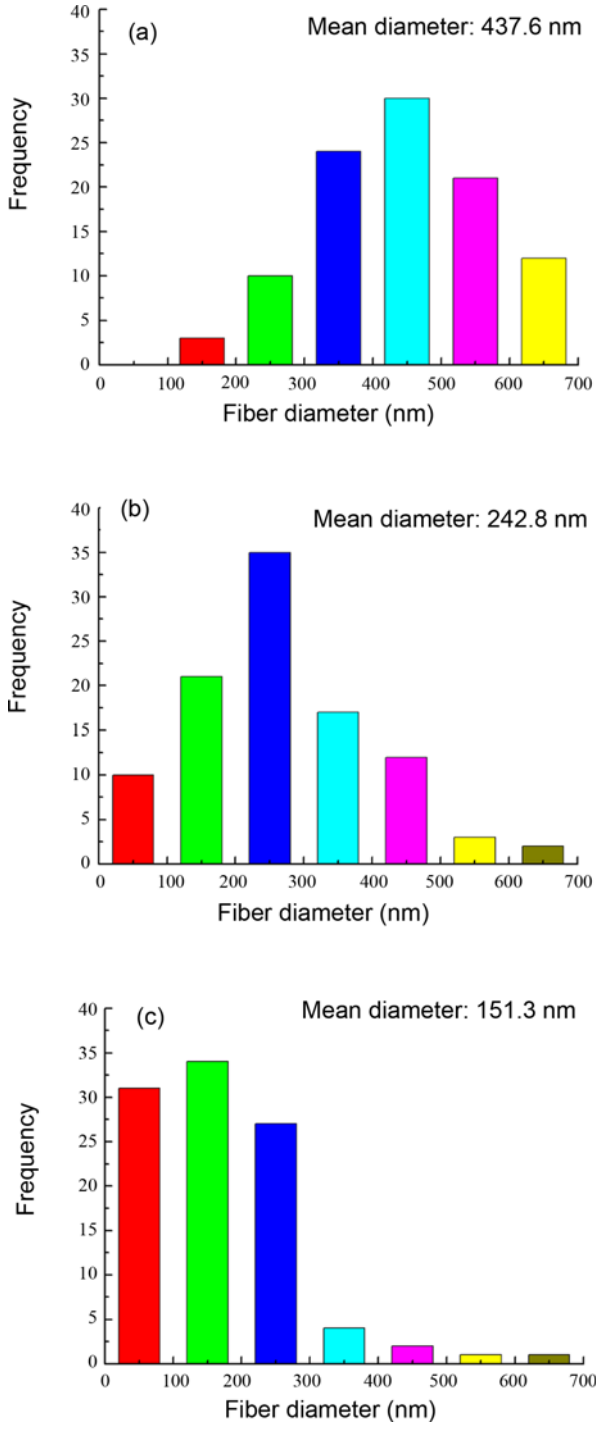

Figure 8. Diameter distributions of the nanofibers obtained under the air pressure of (a) 0.4 MPa, (b) 0.6 MPa, and (c) 0.8 MPa.

Fiber Morphology

SEM photographs of PAN nanofibers prepared under different air pressure and their diameter distributions are shown in Figure 7 and Figure 8. It was evident that average diameter decreased from 437.6 nm to 151.3 nm when the air pressure increased from 0.4 to 0.8 MPa. The spinning solution in the center or at the edge of the flow field suffered different air force because of the distribution characteristics of the flow field, and the uneven distribution of fibers diameter was observed. Nanofibers obtained at 0.4 MPa air pressure, having a broader diameter distribution, mostly presented slightly flat morphology with a greater diameter of 500 nm, except for a few thinner nanofibers around 100 nm in diameter. However, when the air pressure was 0.8 MPa, thinner cylindrical nanofibers with a diameter of 100 nm accounted for the majority. There all existed some thicker nanofibers with a diameter of above 600 nm under the three air pressures because of uneven size of atomized droplets. Compared to needle electrospinning, this novel method could prepare nanofibers with lower diameter and higher production under a relatively lower voltage.

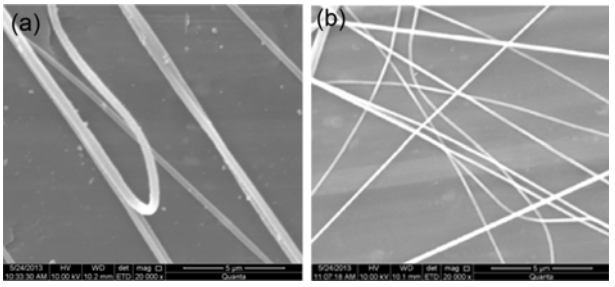

Figure 9. SEM images of the nanofibers; (a) without a 700 mesh filter embedded in the inner wall of the nozzle and (b) with a 700 mesh filter embedded in the inner wall of the nozzle.

The SEM images of the nanofibers with and without a 700 mesh filter embedded in the inner wall of the nozzle had been contrasted and shown in Figure 9. It can be seen that the diameter of the nanofibers prepared under the two kinds of conditions were obviously different. The nanofibers with filter were thinner. Obviously, the filter embedded in the inner wall of the nozzle played an important role in the high pressure air-jet atomized electrospinning.

Forming Mechanism and Process of Nanofibers

The products were collected at different locations from 3 to 50 cm away from the spray nozzle, as shown in Figure 10. It was seen that ellipsoidal droplets with 5 μm diameter appeared at a location from 3 cm away from the nozzle, which were products of airflow atomization. The products collected at the distance of 5 cm were like spindle with short-tails because of a higher initial velocity of the atomized droplets and the volatility of surface solvents due to the air friction. The droplets were continuously elongated and thinned to form nanofibers as the result of the synergetic effect of the electric force and air-drag force with the increase of distance.

It is a longer period for conventional needle electrospinning to form nanofibers because of the slow evolution of Taylor cone from solution droplets. Generally, polymer solution

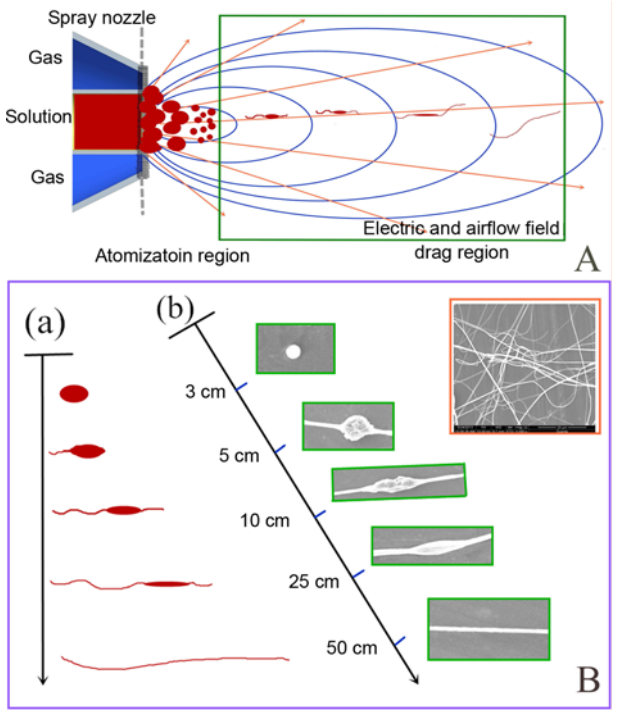

Figure 10. Schematic diagrams of high pressure air-jet atomized electrospinning for the mass production of nanofibers. (A) Schematic illustration of the droplets directly drafting spinning process and (B) proposed mechanism to explain the formation of nanofibers in the high pressure air-jet atomized electrospinning process. (a) Schematic illustrations showing the development from the original droplets to nanofibers and (b) scanning electron micrographs of the nanofiber (or droplet) collected at different locations from 3 to 60 cm away from the spray nozzle.

with high concentration is adopted to make its viscosity be suitable in the range of needle electrospinning, for example, solution concentration about 15 wt% needs to be applied for electrospinning of PAN solution.

Though the flow rate in needle electrospinning was just 0.01-0.1 g/h [19], it usually suffered the problem of needle clogging. Here PAN solution with only 7 wt% concentration was adopted in this novel electrospinning. The spinning solution with lower concentration has lower viscosity, which is easily to be crushed and atomized into massive smaller droplets after being cutted by a filter. Nanofibers drawn from those smaller droplets directly may ensure the spinning continuously. A great flow of 1500 m*l*/h was applied in this electrospinning and the ultrahigh production of 75.6 g/h was up to thousands of times of needle electrospinning.

Conclusion

A novel high pressure air-jet atomized electrospinning was successfully used to produce nanofibers with ultrahigh production. The distribution of flow field under different air pressure was simulated and applied to analyze its effect on the formation of nanofibers. It was found that nanofibers could be prepared directly from massive smaller droplets, which were obtained by crushing and atomizing micron-sized droplets that acquired by cutting lower concentration solution with a filter. When the applied voltage and the distance between nozzle and collector remained constant, the production of nanofibers increased and the diameter of fibers reduced with the air pressure increasing. When 0.8 MPa air pressure was adopted, the production of nanofibers was up to 75.6 g/h, thousands of times of needle electrospinning. This novel electrospinning provides a new approach for mass preparation of nanofibers.

Acknowledgments

This work was supported by a grant from National Natural Science Foundation of China (No. 51203196), and the financial support of the United Foundation from National Natural Science Foundation of China and The People's Government of Henan Province for Cultivating Talents (No. U1204510) is gratefully acknowledged.

References

1. P. P. Tsaia, S. H. Gibson, and P. Gibson, *J. Electrostatics,* **54**, 333 (2002).
2. Z. M. Huang, Y. Z. Zhang, M. Kotaki, and S. Ramakrishna, *Compos. Sci. Technol*., **6**, 2223 (2003).
3. E. Kenawy, K. Mansfield, G. L. Bowlin, D. G. Simpson, and G. E. Wnek, *J. Contr. Release*, **81**, 57 (2002).
4. F. L. Zhou, R. H. Gong, and I. Porat, *Polym. Int.*, **58**, 331 (2009).
5. S. A. Theron, A. L. Yarin, E. Zussman, and E. Kroll, *Polymer*, **46**, 2889 (2005).
6. D. H. Reneker and A. L. Yarin, *Polymer*, **49**, 2387 (2008).
7. B. Ding, E. Kimura, T. Sato, S. Fujita, and S. Shiratori, *Polymer*, **45**, 1895 (2004).
8. O. O. Dosunmu, G. G. Chase, W. Kataphinan, and D. H. Reneker, *Nanotechnology*, **17**, 1123 (2006).
9. J. S. Varabhas, G. G. Chase, and D. H. Reneker, *Polymer*, **49**, 4226 (2008).
10. S. A. Theron, E. Zussman, and A. L. Yarin, *Polymer*, **45**, 2017 (2004).
11. R. R. Yang, J. H. He, L. Xu, and J. Y. Yu, *Polymer*, **50**, 5846 (2009).
12. D. Lukas, A. Sarkar, and P. Pokorny, *J. Appl. Phys.,* **103**, 084309 (2008).
13. A. Valipouri, S. A. H. Ravandi, and A. R. Pishevar, *Fiber. Polym.*, **14**, 941 (2013).
14. Y. Y. Yao, P. X. Zhu, H. Ye, A. J. Niu, X. S. Gao, and D. C. Wu, *Acta Polymerica Sinica*, **1**, 687 (2005).
15. B. M. Tudorel, L. Ignat, B. M. Iulia, and M. Pinteala, *Fiber. Polym.*, **14**, 1526 (2013).

16. Y. Zou, C. Y. Cheng, J. Chen, A. Greiner, and H. Q. Hou, *Polym. Mater. Sci. Eng.*, **100**, 490 (2009).
17. H. Y. Hsiao, C. M. Huang, Y. Y. Liu, Y. C. Kuo, and H. Chen, *J. Appl. Polym Sci.*, **124**, 4904 (2012).
18. Z. Eduard, D. Cho, and Y. L. Joo, *Polymer*, **51**, 4140 (2010).
19. W. E. Teo, R. Gopal, R. Ramaseshan, K. Fujihara, and S. Ramakrishna, *Polymer*, **48**, 34 (2007).